

1 **Refined mapping of tree cover at fine-scale using time-series**
2 **Planet-NICFI and Sentinel-1 imagery for Southeast Asia (2016-**
3 **2021)**

4 Feng Yang^a, Zhenzhong Zeng^{a, *}

5 ^a School of Environmental Science and Engineering, Southern University of Science and Technology,
6 Shenzhen 518055, China

7

8

9 * Correspondence to: zengzz@sustech.edu.cn (Zhenzhong Zeng)

10 Mailing Address:

11 College of Engineering N808

12 Southern University of Science and Technology

13 Shenzhen, China

14

15

16

17 The manuscript for *Earth System Science Data*

18 August 12, 2023

19

20 **Abstract:**

21 High-resolution mapping of tree cover is indispensable for effectively addressing tropical forest carbon loss,
22 climate warming, biodiversity conservation, and sustainable development. However, the availability of
23 precise high-resolution tree cover map products remains inadequate due to the inherent limitations of
24 mapping techniques utilizing medium-to-coarse resolution satellite imagery, such as Landsat and Sentinel-2
25 imagery. In this study, we have generated an annual tree cover map product at a resolution of 4.77 m for
26 Southeast Asia (SEA) for the years 2016-2021 by integrating Planet-Norway's International Climate &
27 Forests Initiative (NICFI) imagery and Sentinel-1 Synthetic Aperture Radar data. We have also collected
28 annual tree cover/non-tree cover samples to assess the accuracy of our Planet-NICFI tree cover map product.
29 The results show that our Planet-NICFI tree cover map product during 2016-2021 achieve high accuracy,
30 with an overall accuracy of $\geq 0.867 \pm 0.017$ and a mean F1 score of 0.921, respectively. Furthermore, our tree
31 cover map product exhibits high temporal consistency from 2016 to 2021. Compared to existing map products
32 (FROM-GLC10, ESA WorldCover 2020 and 2021), our tree cover map product exhibits better performance,
33 both statistically and visually. Yet, the imagery obtained from Planet-NICFI performs less in mapping tree
34 cover in areas with diverse vegetation or complex landscapes due to insufficient spectral information.
35 Nevertheless, we highlight the capability of Planet-NICFI imagery in providing quick and fine-scale tree
36 cover mapping to a large extent. The consistent characterization of tree cover dynamics in SEA's tropical
37 forests can be further applied in various disciplines. Our data from 2016 to 2021 at a 4.77 m resolution are
38 publicly available at <https://cstr.cn/31253.11.sciencedb.07173> (Yang and Zeng, 2023).

39

40 **1 Introduction**

41 Forests and tree-based systems outside forests play a crucial role in land-based carbon emissions or removals,

42 making them essential for supporting and monitoring the implementation of the Reducing Emissions from
43 Deforestation and Forest Degradation (REDD+) and other land-based activities under the Paris Agreement
44 (Skea et al., 2022; CoP26, 2021; FAO, 2020). However, current forest cover map products exhibit large errors
45 in accurately estimating forest area and change, particularly in areas such as trees outside forests and forest
46 edge landscapes (Mugabowindekwe et al., 2023; Reiner et al., 2023; Brandt et al., 2020). As a result, there is
47 a growing demand for timely, high-quality, and high-resolution tree cover map products to accurately capture
48 the dynamics and changes in forest cover.

49
50 Many tree cover map products have been developed at medium-to-coarse resolutions (10-500 m), such as
51 Finer Resolution Observation and Monitoring of Global Land Cover 10 m (FROM-GLC10; Gong et al.,
52 2019), Environmental Systems Research Institute (ESRI) Land Cover (2017-2021) (Karra et al., 2021),
53 European Space Agency (ESA) WorldCover 2020 and 2021 (Zanaga et al., 2022; Zanaga et al., 2021), GFC
54 (Hansen et al., 2013), Globeland30 (Chen et al., 2015), Copernicus Global Land Service (CGLS) Land Cover
55 (Buchhorn et al., 2020), ESA Climate Change Initiative (CCI) (ESA, 2017) and the National Aeronautics and
56 Space Administration (NASA) MCD12Q1 (Friedl and Sulla-Menashe, 2019). However, accurate high-
57 resolution tree cover map products at continental-to-global scales are still lacking due to mapping through
58 medium-to-coarse resolution imagery (Zanaga et al., 2021; Hansen et al., 2010). Consequently, some
59 uncertainties occur in acquiring global tree inventories and monitoring forest disturbances (deforestation and
60 forest degradation). This is mainly due to isolated trees or long narrow forest cover removal (Reiner et al.,
61 2023; Wagner et al., 2023; Sexton et al., 2016; Hammer et al., 2014; Hsieh et al., 2001).

62
63 Only recently have two tree cover map products at <4.77 m been produced over Africa and the state of Mato

64 GROSSO in Brazil using Planet-Norway's International Climate & Forests Initiative (NICFI) imagery based on
65 deep learning algorithms (Reiner et al., 2023; Wagner et al., 2023). However, these two maps have only
66 limited temporal or spatial coverage that occurred. Since the early 21st century, agricultural expansion has
67 created a new wave of drastic land use/land cover changes in Southeast Asia (SEA), leading the region to be
68 one of the most deforested regions worldwide (Zeng et al., 2018a; Zeng et al., 2018b; Achard et al., 2014).
69 Average elevations and slopes of forest loss sites have significantly increased in SEA, particularly in the
70 2010s, geometrically irregular upland land use sites commonly occur (Velasco et al., 2022; Feng et al., 2021).
71 However, existing tree cover map products have underestimated deforestation (25-116%) and upland
72 agricultural expansion rates (9-113%), especially on the topographic boundaries in SEA (Zeng et al., 2018a).
73 Thus, fine-resolution tree cover map products in SEA, with high spatial resolution and longer consistent time
74 series, are urgently needed to accurately monitor tree cover loss and related illegal deforestation. In addition,
75 combining high-resolution optical imagery and Synthetic Aperture Radar (SAR) data (e.g., Sentinel-1) to
76 produce large-area tree cover map products is still in its early stage (Zanaga et al., 2022; Karra et al., 2021;
77 Zanaga et al., 2021; Buchhorn et al., 2020; Hansen et al., 2010).

78

79 Concurrently, advances in large-scale cloud computing (e.g., Google Earth Engine, GEE; Gorelick et al.,
80 2017) and available high-resolution satellite imagery (Roy et al., 2021) can facilitate the development of
81 high-resolution and longer time-series tree cover map products at continental-to-global scales. In this paper,
82 we generated a state-of-the-art fine-scale open-source tree cover map product for SEA during 2016-2021
83 using Planet- NICFI imagery, Sentinel-1 SAR data, and the random forest (RF) method from a previous study
84 (Yang et al., 2023). This dataset allows for extensive assessments of forest dynamics change, such as
85 deforestation, forest degradation, and reforestation. In addition, our dataset can monitor trees outside forests

86 and long narrow forest cover removal, thus improving the accuracy of automated continental tree inventories,
87 which helps optimize REDD+ under the Paris Agreement.

88

89 **2 Materials and methods**

90 **2.1 Satellite imagery**

91 We utilized Planet-NICFI and Sentinel-1 imagery for the years 2016-2021 to generate a time series tree cover
92 map product for SEA. The Planet-NICFI program provides high-resolution (4.77 m per pixel) optical
93 PlanetScope surface reflectance mosaics specifically designed for the tropics. These mosaics offer accurate
94 and reliable spatial data with minimized effects from atmosphere and sensor characteristics, making them an
95 ideal 'ground truth' representation (Planet Team, 2017). The mosaics cover the best imagery to represent every
96 part of the coverage area during leaf-on periods from June to November based on cloud cover and acutance
97 (image sharpness). The Planet-NICFI imageries consist of four bands: red, green, blue, and near-infrared, and
98 cover a time period from 2015 to 2020 at bi-annual resolution for the archive, and from 2020 to 2023 at
99 monthly resolution for monitoring purposes. We accessed and utilized these products in the GEE platform by
100 authorizing our NICFI account to the GEE account.

101

102 We utilized Sentinel-1 on the GEE platform, specifically the 10 m resolution dual-polarization Ground Range
103 Detected (GRD) scenes (VV + VH). We chose Sentinel-1 SAR imagery to correct cases of overestimation
104 caused by confusion with herbaceous vegetation, or underestimation due to optical satellite observations
105 omitting deciduous or semi-deciduous characteristics (Shimada et al., 2014). The SAR imagery, available
106 every 12 days for a single satellite or 6 days for a dual-satellite constellation from October 2014 to the present,
107 was pre-processed with the Sentinel-1 Toolbox for thermal noise removal, radiometric calibration, and terrain

108 correction.

109

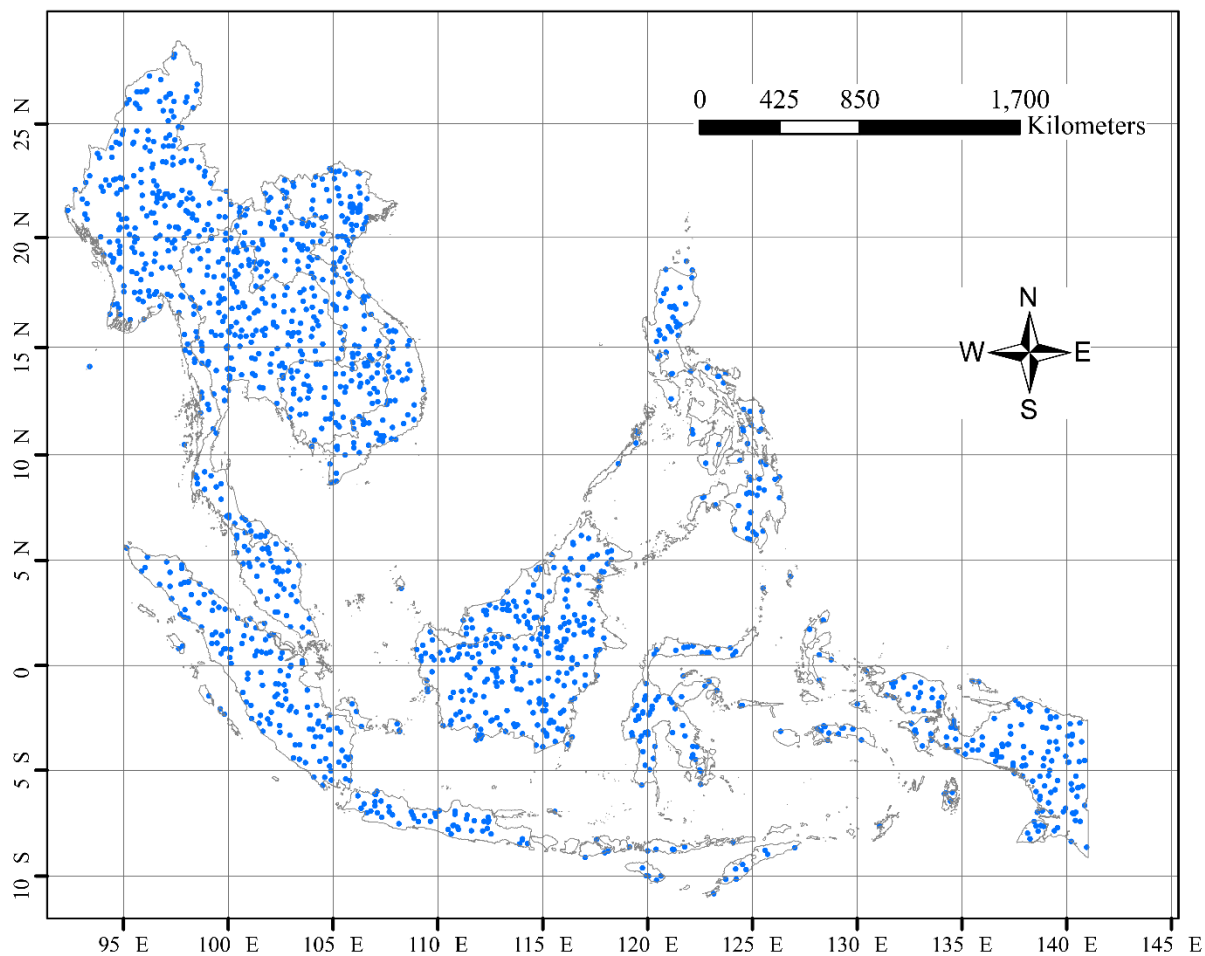
110 **2.2 Validation dataset collection**

111 We collected time series validation datasets to assess the tree cover map product during 2016-2021, except
112 for 2019 as it has been provided by Yang et al. (2023). Our mapping approach has been comprehensively
113 assessed after being developed in 2019 (Yang et al., 2023). However, despite the advancements in the Land
114 Cover Land Use Change (LCLUC) community, a notable gap remains the absence of publicly available high-
115 resolution (e.g., ≤ 10 m) tree cover/non-tree cover labels. The existing coarse-resolution labels for tree
116 cover/non-tree cover can introduce considerable uncertainties when evaluating high-resolution tree cover
117 maps. As a result, our ability to delve deeper into the accuracy of time-series tree cover map datasets was
118 hindered.

119

120 Following the methodology established by Yang et al. (2023), we undertook a rigorous process to generate a
121 robust validation dataset for our study. Firstly, we randomly generated 1,515 points to ensure a representative
122 sample of collected visual data, as illustrated in Fig. 1. Next, to classify these points as trees or non-trees, we
123 enlisted four human interpreters and employed Planet Explorer within QGIS. Our approach involved visually
124 identifying tree cover/non-tree cover pixels in the true color composite of Planet-NICFI imagery where the
125 points were located. To ensure accuracy, we superimposed the 10 m tree height data, previously developed
126 by Lang et al. (2022), onto the Planet-NICFI imagery. This step ensured that the labels adhered to the specified
127 tree height criteria (i.e., ≥ 5 m). Subsequently, we thoroughly evaluated and refined the labels using Google
128 Earth. To make time series tree cover/non-tree cover labels, we maintained the geographic location of the
129 1,515 points and changed the year of the Planet-NICFI imagery. The resulting labels encompassed data from

130 the years 2016, 2017, 2018, 2020, and 2021. Detailed information about the validation dataset can be
 131 presented in Table 1.



132
 133 **Figure 1.** Spatial distribution of randomly generated 1,515 validation dataset points.

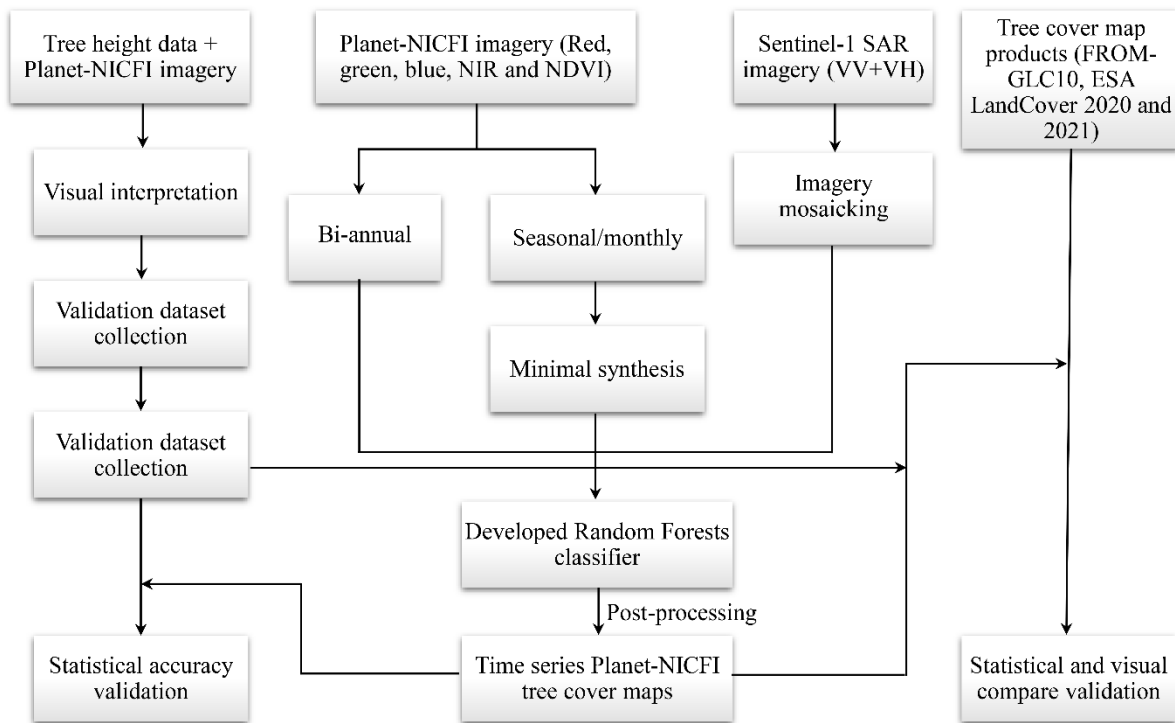
134
 135 **Table 1** Information of the mapped validation dataset for evaluating the generated tree cover map product.

Period	Count of sample points		
	Tree cover	Non-tree cover	Total
2016	1,086	429	1,515
2017	1,026	489	1,515
2018	977	538	1,515
2020	1,093	422	1,515
2021	952	563	1,515

136

137 **2.3 Methods**

138 We integrated Planet-NICFI and Sentinel-1 SAR imagery to generate a high-resolution (4.77 m) annual tree
139 cover map product for SEA covering the years 2015-2021. Our framework involved several key steps,
140 including defining mapped objects, preprocessing of imagery, and generation of time-series tree cover map
141 product. The detailed workflow is illustrated in Fig. 2.



142
143 **Figure 2.** Workflow of generating tree cover map product for 2016-2021, including imagery preprocessing,
144 generation of tree cover map product, and accuracy validation.

145
146 **2.3.1 Definition of mapped tree cover**

147 Traditionally, forests are considered to meet specific criteria (tree cover and height). The Food and Agriculture
148 Organization (FAO) of the United Nations defines forests as land spanning more than 0.5 hectares with trees
149 higher than 5 m and a canopy cover above 10% (FAO, 2020). According to the United Nations Framework
150 Convention on Climate Change (UNFCCC), forests are defined as areas with a minimum canopy cover of
151 10-30%, minimum tree height of 2-5 m, and a minimum area of 0.1 ha (Parker et al., 2008).

152

153 In this study, tree cover is defined as any geographic area dominated by trees without a percentage of tree
154 coverage at the pixel level (Zanaga et al., 2020; Hansen et al., 2013). This is attributed to the fact that the
155 resolution of the Planet pixel (4.77 m) is closer to the size of trees in tropical areas. Next, we utilized Planet-
156 NICFI imagery to generate only a prototype tree cover map with a resolution of 4.77 m and trees higher than
157 5 m. Our tree cover map product serves as baseline data for forest cover analysis. Upon further development
158 of the map to include trees higher than 5/2-5 m, it can be utilized for deriving forest cover maps for various
159 functions, such as those provided by FAO and UNFCCC.

160

161 2.3.2 Preprocessing of imagery

162 We utilized the GEE platform to preprocess Planet-NICFI imagery and Sentinel-1 SAR data for generating
163 tree cover maps for the years 2016-2021 (Fig. 2). Specifically, following the methodology of Yang et al.
164 (2023), we first employed the `ee.ImageCollection.mosaic()` function to merge and assemble overlapping
165 Sentinel-1 SAR data over the specified time period into a seamless, continuous imagery. Subsequently, we
166 performed bilinear resampling on the SAR imagery, specifically the VV and VH bands, to match the spatial
167 resolution of Planet-NICFI imagery with a spatial resolution of 4.77 m.

168

169 Planet-NICFI offers imagery at two different temporal frequencies spanning from 2016 to 2021. This includes
170 semi-annual imagery from 2016 to 2019 and monthly data from 2020 to 2021. To create a coherent and
171 consistent dataset for 2020 and 2021, we synthesized the selected time window of monthly imagery into
172 single imagery for each band, namely red, green, blue, and near-infrared bands. Specifically, we utilized the
173 `ee.ImageCollection.min()` function on each monthly imagery to extract the minimum monthly imagery, which

174 was then used to generate the second semi-annual imagery for 2020 and 2021. This approach was employed
175 to minimize the impact of cloud pollution on Planet-NICFI imagery (Oishi et al, 2018).

176

177 2.3.3 Generation of time-series tree cover map product

178 In addition to applying the RF approach in our tree cover mapping (Yang et al., 2023), RF-based methods
179 have been widely employed to develop global LCLUC products and show good performance (Zanaga et al.,
180 2022; Zanaga et al., 2021; Buchhorn et al., 2020). To acquire the time-series tree cover map dataset, our
181 methodology involved a two-step process. Initially, we integrated our custom RF approach, implemented on
182 Google Earth Engine (GEE), with a cloud-based machine learning platform. This combination enabled us to
183 obtain semi-annual Planet-NICFI and Sentinel-1 imageries spanning the years 2016 to 2021, as illustrated in
184 Fig. 2. Following data acquisition, we performed several post-processing steps to generate accurate tree cover
185 map product for the SEA region. These steps included downloading the acquired data from the cloud platform
186 to a local location, conducting mosaic operations, clipping relevant areas, applying projection transformations,
187 and performing correlation statistics. By employing this approach, we produced a high-resolution tree cover
188 map product.

189

190 2.3.4 Statistical accuracy assessment

191 We used two methods to assess the statistical accuracy of our tree cover map product. The generated tree
192 cover map product was compared pixel by pixel with the tree cover/non-tree cover labels. We then obtained
193 a confusion matrix, including true tree cover (TP), true non-tree cover (TN), false tree cover (FP), and false
194 non-tree cover (FN). These four values were used to calculate the user's accuracy, producer's accuracy, and
195 overall accuracy at a 95% confidence level (Olofsson et al., 2014) and the F1 score based on Eqs. (1)-(4),
196 respectively. Note that we opted against utilizing the Kappa coefficient for accuracy assessment due to its

197 unsuitability for mapping error evaluation (Pontius Jr et al., 2011; Allouche et al., 2006).

$$\text{User's accuracy (UA)} = \frac{TP}{TP + FP} \quad (1)$$

$$\text{Producer's accuracy (PA)} = \frac{TP}{TP + FN} \quad (2)$$

$$\text{Overall accuracy} = \frac{TP + TN}{TP + TN + FP + FN} \quad (3)$$

$$\text{F1 score} = \frac{2 \times UA \times PA}{UA + PA} \quad (4)$$

198

199 In addition, following Tsendbazar et al. (2021), we used a stability index based on the user's and producer's

200 accuracy to evaluate the time-series accuracy consistency of the tree cover map product. The stability index

201 used to evaluate tree cover accuracy is expressed as

$$SI_{t1} = \frac{|TC_{t1} - TC_{t1-1}|}{TC_{t1-1}} \times 100 \quad (5)$$

202 where SI_{t1} is the stability index that indicates the accuracy of tree cover maps (user's or producer's accuracy)

203 at time $t1$, TC_{t1} is tree cover accuracy at time $t1$ and TC_{t1-1} is tree cover accuracy at the previous time ($t0$

204 or the reference year). We also used the maximum and average stability index for two consecutive years to

205 assess the stability of our tree cover map product over a long period.

206

207 **3 Results**

208 We employed two approaches to assess the performance of our Planet-NICFI 2016-2021 tree cover map

209 product. Firstly, we estimated the accuracy of our tree cover map product for each year to gain insights into

210 their accuracy and consistency, based on the method developed by Tsendbazar et al. (2021). Additionally, we

211 presented illustrative time series tree cover maps and documented the dynamics in tree cover area changes

212 during the 2016-2021 period. Secondly, we compared our tree cover map product to widely used global tree

213 cover map products at 10 m resolution, including FROM-GLC10 in 2017 (Gong et al., 2019), as well as ESA

214 WorldCover 2020 and 2021 (Zanaga et al., 2022; Zanaga et al., 2021).

215

216 3.1 Assessment of tree cover map product

217 We reported the annual accuracy of the time-series Planet-NICFI tree cover map product in Table 2 with a
218 95% confidence level. The tree cover accuracy results for 2019 were provided by Yang et al. (2023). The
219 overall accuracy of the tree cover map product ranged between $0.867-0.907 \pm 0.015$ from 2016 to 2021, with
220 the highest accuracy of 0.907 ± 0.014 in 2021 and the lowest accuracy of 0.867 ± 0.017 in 2016 (Table 2). This
221 discrepancy may be due to poor data in the Planet-NICFI imagery during 2016 (Roy et al., 2021). The F1
222 score showed a similar trend from 2016 to 2021, with an average of approximately 0.921. The user's accuracy
223 consistently exceeded 0.901 ± 0.017 over the six years, except for 2016 when it was 0.862 ± 0.021 . The
224 producer's accuracies were all higher than 0.912 ± 0.014 (Table 2). Nevertheless, the mapping results of our
225 time-series Planet-NICFI tree cover maps were highly consistent. Additionally, compared to the tree cover,
226 the non-tree cover showed lower user's accuracy, producer's accuracy, and F1 score (i.e., approximately
227 0.856 ± 0.027 , 0.852 ± 0.025 , and 0.853, respectively), likely due to the complex composition of non-tree cover
228 types, such as shrubland and herbaceous wetland.

229

230 **Table 2** User's accuracies, producer's accuracies, F1 score, and overall accuracies of the Planet-NICFI V1.0
231 2016-2021 tree cover map product for SEA at a 95% confidence level. The accuracy evaluation results in
232 2019 were provided by Yang et al. (2023).

Year	Classification	User's accuracy	Producer's accuracy	F1 score	Overall accuracy
2016	Tree cover	0.862 ± 0.021	0.925 ± 0.018	0.892	0.867 ± 0.017
	Non-tree cover	0.876 ± 0.031	0.783 ± 0.026	0.827	
2017	Tree cover	0.901 ± 0.017	0.935 ± 0.016	0.917	0.892 ± 0.016
	Non-tree cover	0.874 ± 0.033	0.814 ± 0.027	0.843	
2018	Tree cover	0.929 ± 0.016	0.912 ± 0.014	0.920	0.892 ± 0.015
	Non-tree cover	0.816 ± 0.033	0.85 ± 0.030	0.832	
2019	Tree cover	0.913 ± 0.012	0.933 ± 0.010	0.923	0.895 ± 0.011
	Non-tree cover	0.857 ± 0.022	0.819 ± 0.021	0.837	

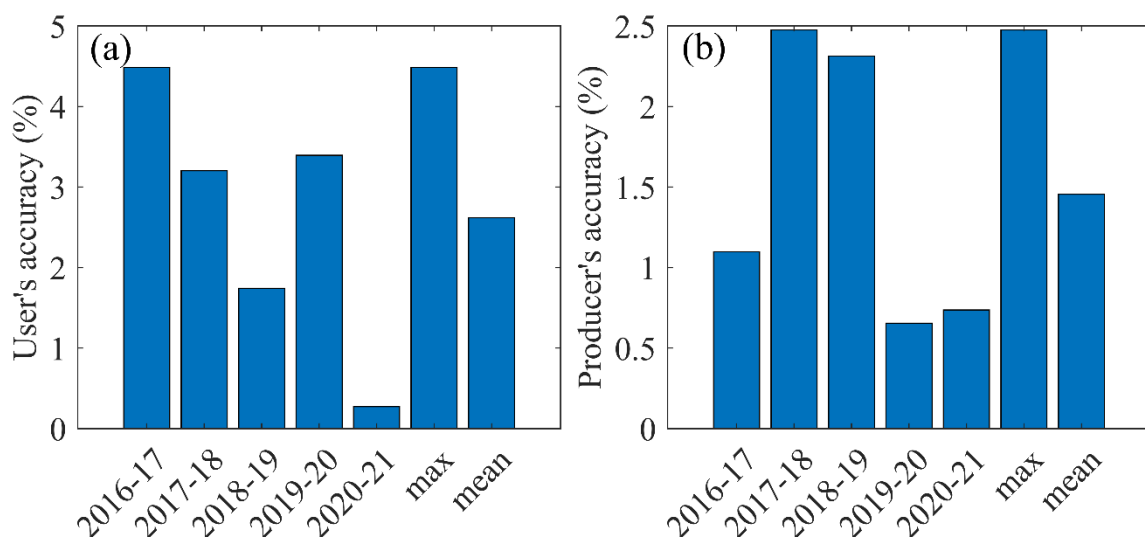
2020	Tree cover	0.944±0.014	0.927±0.011	0.935	0.900±0.014
	Non-tree cover	0.754±0.041	0.803±0.040	0.778	
2021	Tree cover	0.947±0.014	0.934±0.011	0.940	0.907±0.014
	Non-tree cover	0.778±0.038	0.816±0.039	0.796	

233

234 We also estimated the stability of our Planet-NICFI tree cover maps accuracy over 2016-2021 (Fig. 3). The

235 results show that the user's and producer's stability indexes were low than 4.5% and 2.5%, respectively,

236 indicating the good stability of our mapped Planet-NICFI tree cover maps for the six years (2016-2021).



237

238 **Figure 3.** Stability index estimates for the Planet-NICFI tree cover map product 2016-2021: the stability
239 index for (a) the user's accuracy and (b) the producer's accuracy.

240

241 We further visually compared our time-series tree cover map product with the original Planet-NICFI imagery

242 during 2016-2019 (Figures 4-5). Note that we have not shown the years 2020 and 2021 due to inconvenient

243 visualization for monthly resolution Planet-NICFI imagery collected from QGIS. In comparison, our tree

244 cover map product showed better consistencies with Planet-NICFI imagery, such as roads, the spatial

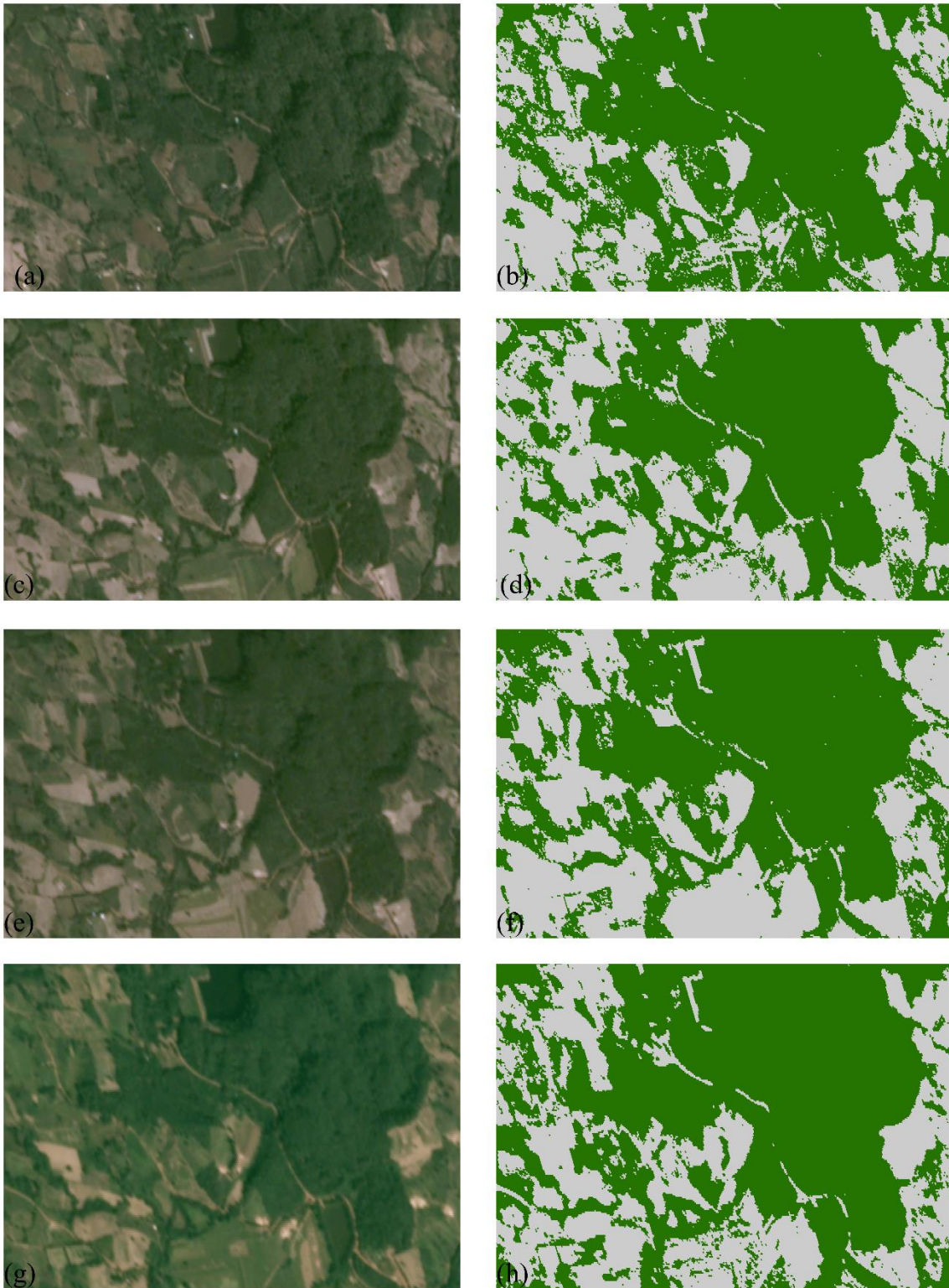
245 distribution pattern of tree cover, and non-tree cover. However, our tree cover product potentially exhibited

246 a "salt and pepper" phenomenon in some years (i.e., 2017 and 2018) due to the employment of the RF

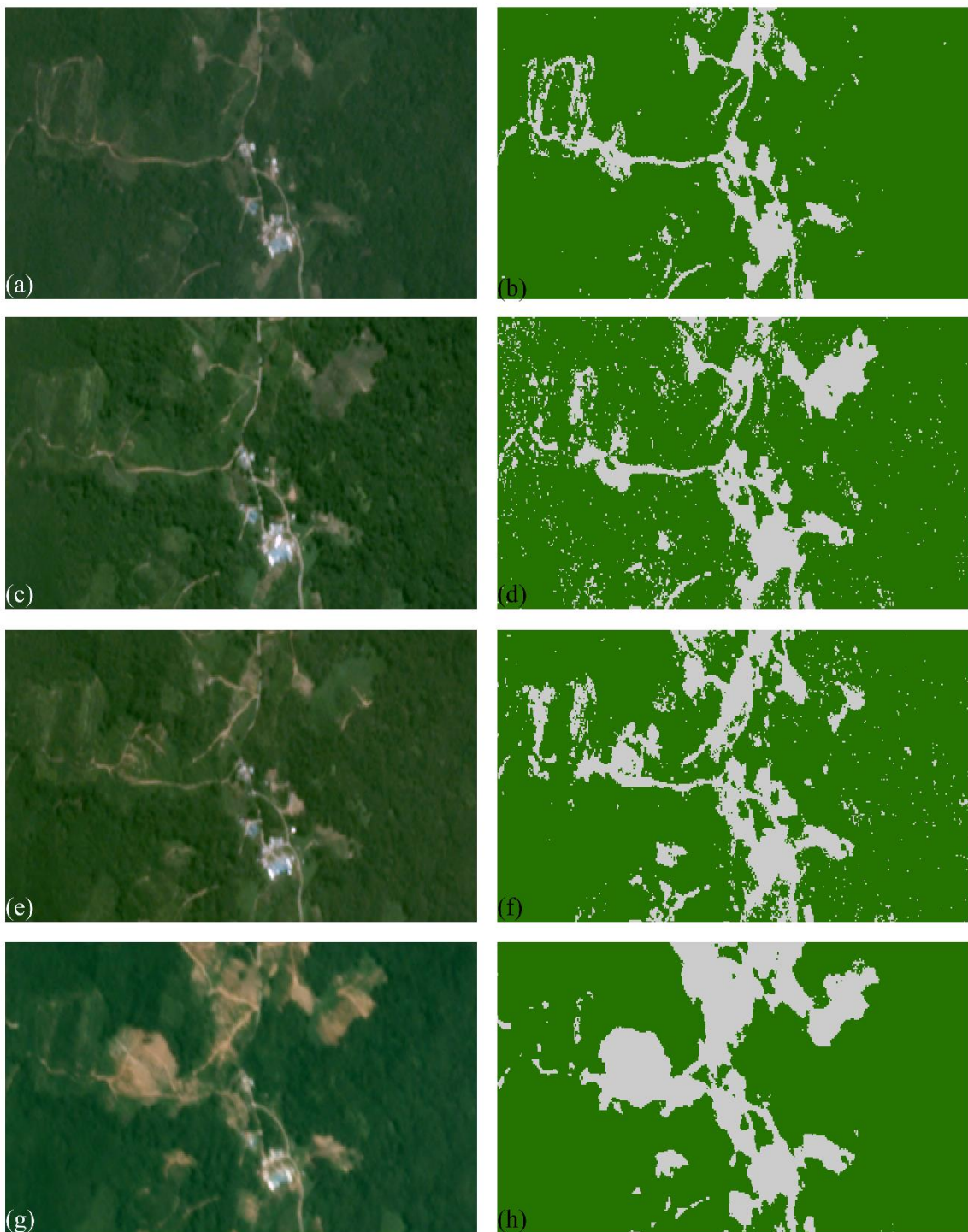
247 approach. In practical applications, we need to pay attention to this phenomenon. In addition, we counted the

248 time series of the area estimates of tree cover maps during 2016-2021 and showed a slight increase trend

249 from 2016 to 2021, which is in line with the area estimates of ESA tree cover for the years 2020 and 2021.
250 This may be due to forest restoration after the 2015 El Niño phenomenon (Wigneron et al., 2020), as well as
251 the impact of expanded plantations (Xu et al., 2020).



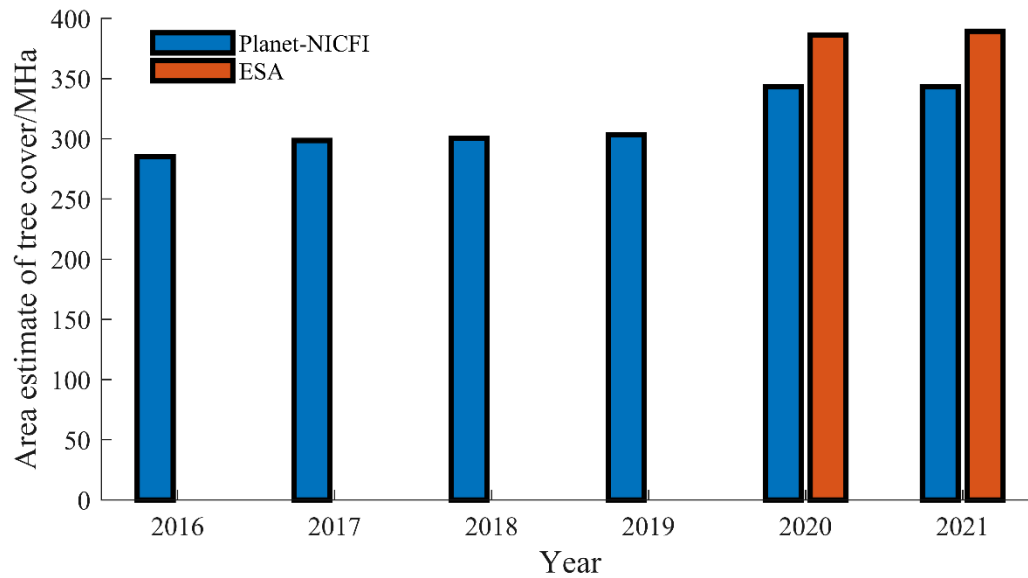
252
 253 **Figure 4.** Comparison of the time series of the derived tree cover maps (left column) and Planet-NICFI
 254 imagery (right column) for the selected mainland SEA area (100.301°-100.322°E, 18.400°-18.409°N). (a)
 255 and (b), (c) and (d), (e) and (f), and (g) and (h) indicate 2019, 2018, 2017, and 2017, respectively.



256

257 **Figure 5.** Comparison of the time series of the derived tree cover maps (left column) and Planet-NICFI
 258 imagery (right column) for the selected maritime SEA area (111.789°-111.806°E, 2.032°-2.040°N). (a) and
 259 (b), (c) and (d), (e) and (f), and (g) and (h) indicate 2019, 2018, 2017, and 2017, respectively.

260

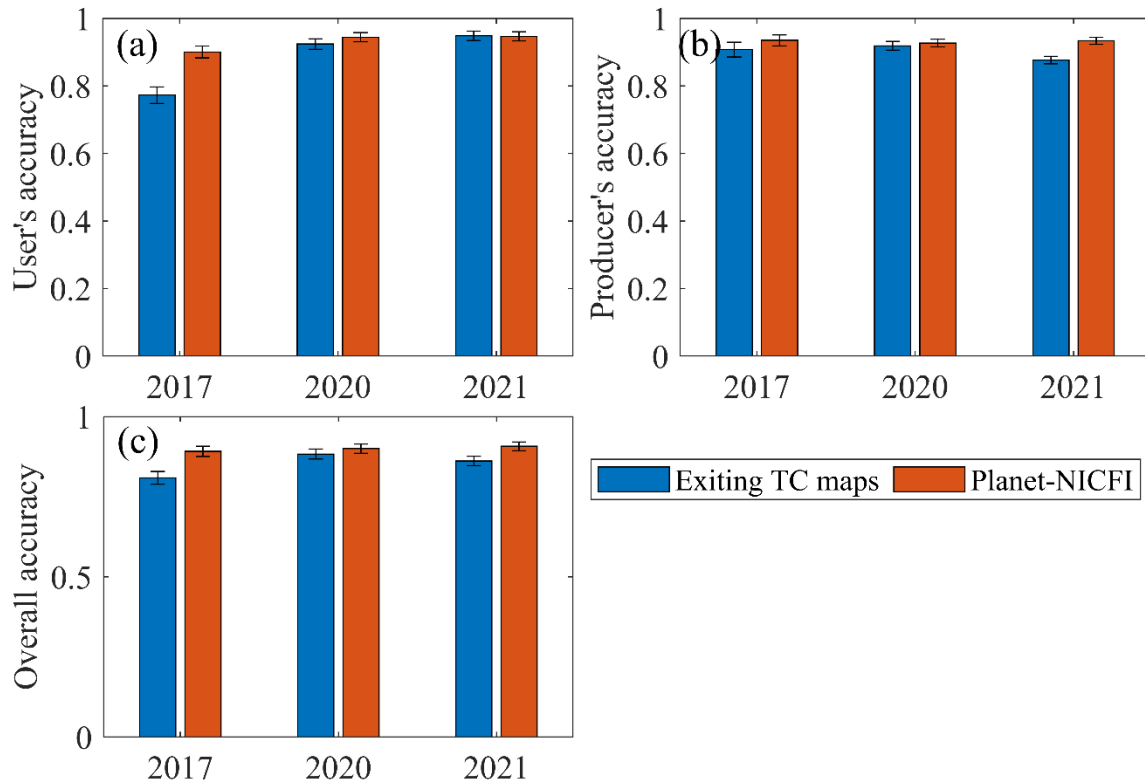


261
 262 **Figure 6.** Area dynamics change of tree cover maps for Planet-NICFI and ESA from 2016 to 2021.

263

264 **3.2 Comparison with existing tree cover map products**

265 We compared our mapped Planet-NICFI tree cover maps with FROM-GLC10, ESA WorldCover 2020 and
 266 2021 regarding statistical accuracy (Fig. 4). The results show that our tree cover maps outperformed FROM-
 267 GLC10 in user’s accuracy, producer’s accuracy, and overall accuracy. The user’s accuracy and overall
 268 accuracy of our tree cover maps exceeded 0.083. ESA WorldCover 2020 and 2021 showed similar
 269 performances to our Planet-NICFI tree cover maps. Particularly, the user’s accuracy, producer’s accuracy,
 270 and overall accuracy of ESA WorldCover 2020 decreased by 0.020, 0.008, and 0.017, respectively (Fig. 4).
 271 This may be because we all used the SAR imagery as input and applied the RF-based machine learning
 272 method to classify our tree cover.



273

274 **Figure 7.** Accuracy comparison between existing tree cover maps and the generated Planet-NICFI tree cover
 275 maps at a 95% confidence level: (a) user's accuracy, (b) producer's accuracy, and (c) overall accuracy.

276

277 We selected six locations (three mainland SEA areas and three maritime SEA areas) to visually compare our

278 Planet-NICFI tree cover maps with three other 10-meter products, namely, FROM-GLC10, ESA WorldCover

279 2020 and 2021 (Figs. 8-10). In comparison, it is easier for FROM-GLC10 to classify all mixed tree and non-

280 tree areas into non-tree cover maps (Fig. 8a). This may be because FROM-GLC10 cannot apply SAR imagery

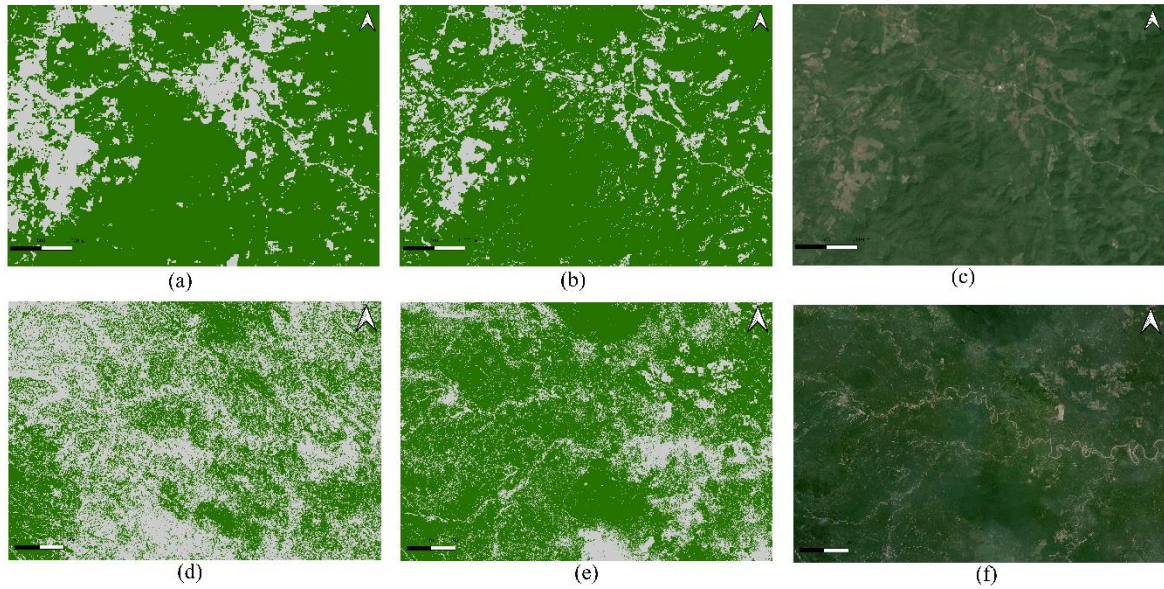
281 to tree cover mapping. However, ESA WorldCover 2020 and 2021 can capture tree cover landscapes at a

282 higher level of detail than FROM-GLC, such as long narrow roads, croplands, and built-up areas (Figs. 9-

283 10a). It should be noted that ESA WorldCover 2020 and 2021 omitted some long narrow non-tree cover

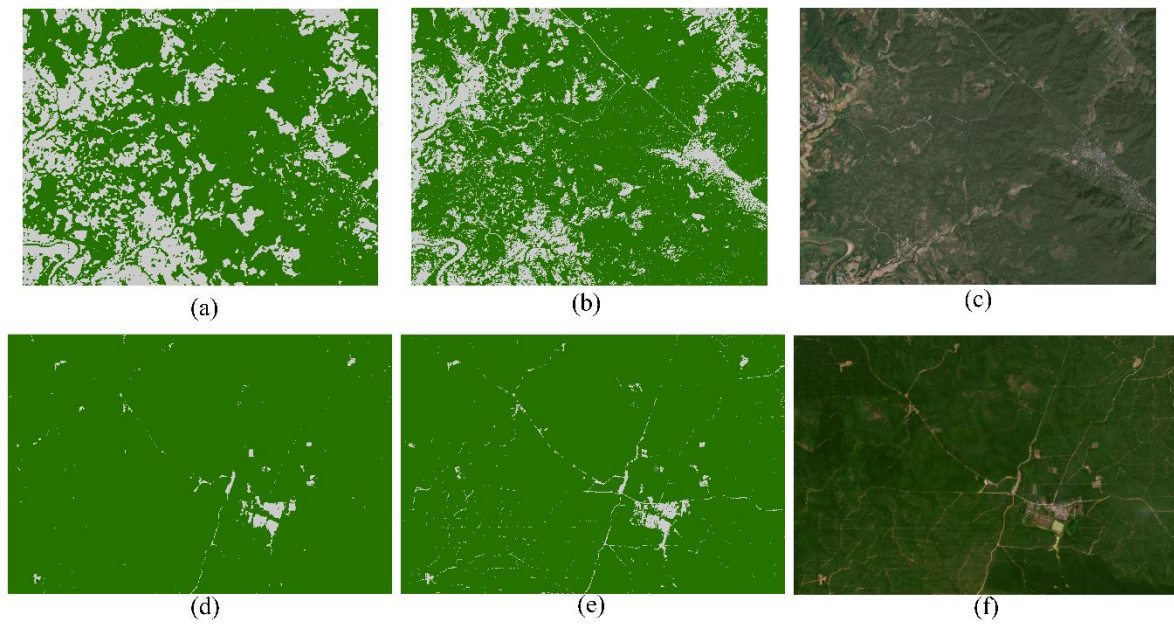
284 landscapes and small isolated tree cover and non-tree cover landscapes due to the limitation of the imagery

285 resolution (10 m).



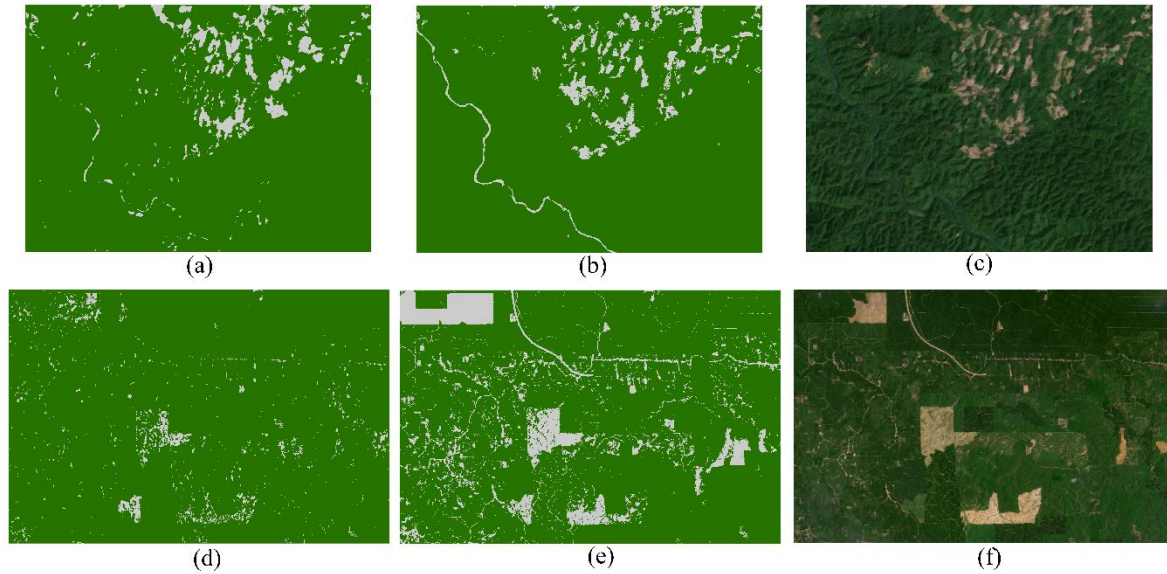
286
287
288
289
290
291

Figure 8. Comparison of FROM-GLC10 (a) and (d), Planet-NICFI tree cover (b) and (e), and Planet-NICFI imagery (c) and (f) for mainland SEA area (101.594°-101.651°E, 19.254°-19.294°N; top row) and maritime SEA area (101.925°-103.296°E, -2.096°-1.145°S; bottom row). Green and gray 20% indicate tree cover and non-tree cover, respectively.



292
293
294
295
296
297

Figure 9. Comparison of ESA WorldCover 2020 (a) and (d), Planet-NICFI tree cover (b) and (e), and Planet-NICFI imagery (c) and (f) for mainland SEA area (98.310°-98.392°E, 17.102°-17.166°N; top row) and maritime SEA area (99.983°-100.064°E, 1.387°-1.442°N; bottom row). Green and gray 20% indicate tree cover and non-tree cover, respectively.



298
 299 **Figure 10.** Comparison of ESA WorldCover 2021 (a) and (d), Planet-NICFI tree cover (b) and (e), and Planet-
 300 NICFI imagery (c) and (f) for Mainland SEA area (102.179°-102.249°E, 18.676°-18.726°N; top row) and
 301 maritime SEA area (99.951°-100.063°E, 1.892°-1.967°E; bottom row). Green and gray 20% indicate tree
 302 cover and non-tree cover, respectively.

303

304 **4 Discussion**

305 Our time-series Planet-NICFI tree cover map product was mapped twice a year to mitigate the impact of
 306 smog, light, cloud, and topographic effects in tropical areas (Roy et al., 2021; Marta et al., 2018). This high-
 307 resolution tree cover map product meets the minimum tree height requirement of ≥ 5 m for further generating
 308 forest data. However, it should be noted that we cannot guarantee 100% tree cover for each higher-resolution
 309 pixel, which may introduce some uncertainties when using the higher-resolution tree cover maps. Despite
 310 excluding plantations during sample point labeling, some plantations, such as oil palm, may still be mixed
 311 into our tree cover map product due to similarities in anomalies (Mugabowindekwe et al., 2023; Zanaga et
 312 al., 2022; Zanaga et al., 2021). As a result, caution should be exercised when using our Planet-NICFI tree
 313 cover map product for certain purposes.

314

315 To generate a high-resolution time series tree cover map product at a continental scale, we utilized advanced

316 random forests-based machine learning algorithms on the GEE platform. However, for fine-scale tree cover
317 mapping, deep learning-based segmentation methods, such as U-net (Falk et al., 2019), are necessary,
318 particularly when using limited bands (Mugabowindekwe et al., 2023; Wagner et al., 2023; Zanaga et al.,
319 2022; Zanaga et al., 2021; Brandt et al., 2020). As a result, our tree cover map product still has some
320 uncertainty due to limitations in the optical PlanetScope imagery. Additionally, our tree cover map product
321 has the potential to display a salt and pepper phenomenon in certain locations and years, attributed to the
322 utilization of the RF method. To improve our tree cover mapping product with higher accuracy, we need to
323 consider adding more bands or utilizing advanced deep learning algorithms in the future.

324

325 **5 Data availability**

326 The high-resolution Planet-NICFI V1.0 time-series tree cover product is now available at
327 <https://cstr.cn/31253.11.sciencedb.07173> (Yang and Zeng, 2023). This product is provided in the Mollweide
328 projection and the World Geodetic System 1984 (WGS1984) datum and geographic coordinate system. Tree
329 cover and non-tree cover are denoted as 0 and 1, respectively, in each yearly file, and are stored as UINT8 in
330 GeoTIFF format. The GeoTIFF files are named Planet-FC_SEA_<YEAR>_prj.tif, for example, Planet-
331 FC_SEA_16_prj.tif.

332

333 **6 Conclusions**

334 We have successfully generated the first accurate and high-resolution time-series tree cover map product for
335 SEA by combining optical and SAR satellite observations, utilizing advanced random forests machine
336 learning algorithms on the GEE platform. Our Planet-NICFI tree cover map product exhibits excellent
337 accuracy and consistency over six years (2016-2021). The baseline tree cover map product, with a resolution

338 of 4.77 m, can be easily converted to forest cover maps at different resolutions to cater to the diverse needs
339 of users. Moreover, our tree cover map product has the unique ability to address rounding errors in forest
340 cover mapping by accurately capturing isolated trees and monitoring the removal of long, narrow forest cover.
341 These cutting-edge fine-scale time-series tree cover maps represent a milestone in forest monitoring and offer
342 unprecedented opportunities for users across diverse disciplines.

343

344 **Code Availability**

345 The scripts used to generate all Planet-NICFI v1.0 tree cover 2016-2021 are provided in JavaScript
346 (https://code.earthengine.google.com/?scriptPath=users%2Fyfhtaurus%2Fcodes%3APlanet_RF-LC_rac).

347 The maps can be automatically generated by running the codes. The scripts are also available on request from
348 Z. Zeng.

349

350 **Acknowledgments**

351 This study was supported by the National Natural Science Foundation of China (grant no. 42071022), the
352 start-up fund provided by the Southern University of Science and Technology (no. 29/Y01296122), and the
353 China Postdoctoral Science Foundation (grant no. 2022M711472). We thank Sen Jiang, Haowen Duan, Hao
354 Li, and Fangdong Fu for making tree cover/non-tree cover label data that are used to assess the time series
355 tree cover map products.

356

357 **Author contributions**

358 Z.Z. designed the research; F.Y. performed the analysis and wrote the draft. All authors contributed to the

359 interpretation of the results and the writing of the paper.

360

361 **Competing interests**

362 The authors declare no competing interests.

363 **References**

- 364 Achard, F., Beuchle, R., Mayaux, P. et al.: Determination of tropical deforestation rates and related carbon
365 losses from 1990 to 2010, *Glob Chang Biol*, 20(8), 2540-2554, 2014.
- 366 Allouche, O., Tsoar, A., Kadmon, R.: Assessing the accuracy of species distribution models: prevalence,
367 kappa and the true skill statistic (TSS), *J. Appl. Ecol.*, 43(6), 1223-1232, 2006.
- 368 Brandt, M., Tucker, C. J., Kariryaa, A., et al.: An unexpectedly large count of trees in the West African Sahara
369 and Sahel, *Nature*, 587(7832), 78-82, 2020.
- 370 Buchhorn, M., Lesiv, M., Tsendbazar, N. E., et al.: Copernicus global land cover layers—collection 2, *Remote*
371 *Sens.*, 12(6), 1044, 2020.
- 372 Chen, J., Chen, J., Liao, A., et al.: Global land cover mapping at 30 m resolution: A POK-based operational
373 approach. *ISPRS J. Photogramm, Remote Sens.*, 103, 7-27, 2015.
- 374 CoP26, G. L.: Glasgow Leaders' Declaration on Forests and Land Use. Available online at: [https://ukcop26.](https://ukcop26.org/glasgow-leaders-declaration-onforests-and-land-use/)
375 [org/glasgow-leaders-declaration-onforests-and-land-use/](https://ukcop26.org/glasgow-leaders-declaration-onforests-and-land-use/)(accessed December 06, 2021).
- 376 ESA: Land Cover CCI Product User Guide Version 2. Tech. Rep. Available at:
377 maps.elie.ucl.ac.be/CCI/viewer/download/ESACCI-LC-Ph2-PUGv2_2.0.pdf, 2017.
- 378 Falk, T., Mai, D., Bensch, R., et al. U-Net: deep learning for cell counting, detection, and morphometry, *Nat.*
379 *Methods*, 16(1), pp.67-70, 2019.
- 380 FAO: Global forest resources assessment 2020: Main report. Technical report, Food and Agriculture
381 Organization of the United Nations, ROME, 2020.
- 382 Feng, Y., Ziegler, A. D., Elsen, P. R., et al.: Upward expansion and acceleration of forest clearance in the
383 mountains of Southeast Asia, *Nat. Sustain*, 4(10), 892-899, 2021.
- 384 Friedl, M., Sulla-Menashe, D.: MCD12Q1 MODIS/Terra+Aqua Land Cover Type Yearly L3 Global 500m
385 SIN Grid V006. NASA EOSDIS Land Processes DAAC. Accessed 2022-12-15 from
386 <https://doi.org/10.5067/MODIS/MCD12Q1.006>, 2019.
- 387 Gong P., Liu H., Zhang M., et al.: Stable classification with limited sample: Transferring a 30-m resolution
388 sample set collected in 2015 to mapping 10-m resolution global land cover in 2017, *Sci. Bull*, 64, 370-
389 373, 2019.
- 390 Gorelick, N., Hancher, M., Dixon, M., et al.: Google Earth Engine: Planetary-scale geospatial analysis for
391 everyone, *Remote Sens. Environ.*, 202, 18-27, 2017.
- 392 Hammer, D., Kraft, R., Wheeler, D.: Alerts of forest disturbance from MODIS imagery, *Int J Appl Earth Obs*
393 *Geoinf*, 33, 1-9, 2014.
- 394 Hansen, M. C., Potapov, P. V., Moore, R., et al.: High-resolution global maps of 21st-century forest cover
395 change, *Science*, 342(6160), 850-853, 2013.
- 396 Hansen, M. C., Stehman, S. V., Potapov, P. V.: Quantification of global gross forest cover loss, *Proc Natl*
397 *Acad Sci USA*, 107(19), 8650-8655, 2010.
- 398 Hsieh, P. F., Lee, L. C., Chen, N. Y.: Effect of spatial resolution on classification errors of pure and mixed
399 pixels in remote sensing, *IEEE Trans. Geosci. Remote Sens.*, 39(12), 2657-2663, 2001.
- 400 Karra K., Kontgis C., Statman-Weil Z., et al.: Global land use/land cover with Sentinel 2 and deep learning.
401 In 2021 IEEE international geoscience and remote sensing symposium IGARSS (pp. 4704-4707), IEEE,
402 2021, July.
- 403 Lang, N., Jetz, W., Schindler, K. Wegner, J. D.: A high-resolution canopy height model of the Earth,
404 [doi:10.48550/arxiv.2204.08322](https://doi.org/10.48550/arxiv.2204.08322), 2022.
- 405 Marta, S.: Planet imagery product specifications, Planet Labs: San Francisco, CA, USA, 91, 2018.

406 Mugabowindekwe, M., Brandt, M., Chave, J., et al.: Nation-wide mapping of tree-level aboveground carbon
407 stocks in Rwanda, *Nat. Clim. Change*, 1-7, 2023.

408 Oishi, Y., Sawada, Y., Kamei, A., et al.: Impact of Changes in Minimum Reflectance on Cloud Discrimination,
409 *Remote Sens.*, 10(5), 693, 2018.

410 Olofsson, P., Foody, G.M., Herold, M., et al.: Good practices for estimating area and assessing accuracy of
411 land change, *Remote Sens. Environ.*, 148, 42-57, 2014.

412 Parker, C., Mitchell, A., Trivedi, M., Mardas, N.: The little REDD book: a guide to governmental and non-
413 governmental proposals for reducing emissions from deforestation and degradation. The little REDD
414 book: a guide to governmental and non-governmental proposals for reducing emissions from
415 deforestation and degradation,
416 http://www.globalcanopy.org/themedia/file/PDFs/LRB_lowres/lrb_en.pdf, 2008.

417 Planet Team: Planet Application Program Interface: In Space for Life on Earth. San Francisco, CA,
418 <https://api.planet.com>, 2017.

419 Pontius Jr, R. G., Millones, M.: Death to Kappa: birth of quantity disagreement and allocation disagreement
420 for accuracy assessment, *Int. J. Remote Sens.*, 32(15), 4407-4429, 2011.

421 Reiner, F., Brandt, M., Tong, X., et al.: More than one quarter of Africa's tree cover found outside areas
422 previously classified as forest, *Nat Commun*, 14, 2258 (2023).

423 Roy, D.P., Huang, H., Houborg, R., Martins, V.S.: A global analysis of the temporal availability of
424 PlanetScope high spatial resolution multi-spectral imagery, *Remote Sens. Environ.*, 264, 112586, 2021.

425 Sexton, J.O., Noojipady, P., Song, X.P., Feng, M., Song, D.X., Kim, D.H., Anand, A., Huang, C., Channan,
426 S., Pimm, S.L., Townshend, J.R.: Conservation policy and the measurement of forests, *Nat. Clim.*
427 *Change*, 6(2), 192-196, 2016.

428 Shimada, M., Itoh, T., Motooka, T., Watanabe, M., Shiraishi, T., Thapa, R., & Lucas, R.: New global
429 forest/non-forest maps from ALOS PALSAR data (2007–2010), *Remote Sens. Environ.*, 155, 13-31,
430 2014.

431 Skea J., Shukla P. R., Reisinger A., et al.: Climate change 2022: Mitigation of climate change, IPCC Sixth
432 Assessment Report, 2022.

433 Tsendbazar, N., Herold, M., Li, L., et al.: Towards operational validation of annual global land cover maps,
434 *Remote Sens. Environ.*, 266, 112686, 2021.

435 Velasco, R.F., Lippe, M., Tamayo, F., et al.: Towards accurate mapping of forest in tropical landscapes: A
436 comparison of datasets on how forest transition matters, *Remote Sens. Environ.*, 274, 112997, 2022.

437 Wagner, F. H., Dalagnol, R., Silva-Junior, C. H., et al.: Mapping Tropical Forest Cover and Deforestation
438 with Planet NICFI Satellite Images and Deep Learning in Mato Grosso State (Brazil) from 2015 to 2021,
439 *Remote Sens.*, 15(2), 521, 2023.

440 Wigneron, J.P., Fan, L., Ciais, P., et al. Tropical forests did not recover from the strong 2015–2016 El Niño
441 event, *Sci. Adv.*, 6(6), p.eaay4603, 2020.

442 Xu, Y., Yu, L., Li, W., et al. Annual oil palm plantation maps in Malaysia and Indonesia from 2001 to 2016,
443 *Earth Syst. Sci. Data*, 12(2), pp.847-867, 2020.

444 Yang, F., Jiang X., Alan D. Ziegler, et al. Improved fine-scale tropical forest cover mapping for Southeast
445 Asia using Planet-NICFI and Sentinel-1 imagery, *J. Remote Sens.*, 0,
446 <https://doi.org/10.34133/remotesensing.0064>, 2023.

447 Zanaga D., Van De Kerchove R., Daems D., et al.: ESA WorldCover 10 m 2021 v200,
448 <https://doi.org/10.5281/zenodo.7254221>, 2022.

449 Zanaga D., Van De Kerchove R., De Keersmaecker W., et al.: ESA WorldCover 10 m 2020 v100,

450 <https://doi.org/10.5281/zenodo.5571936>, 2021.
451 Zeng, Z., Estes, L., Ziegler, A. D., et al.: Highland cropland expansion and forest loss in Southeast Asia in
452 the twenty-first century, *Nat. Geosci*, 11(8), 556-562, 2018a.
453 Zeng, Z., Gower, D. and Wood, E. F.: Accelerating Forest loss in Southeast Asian Massif in the 21st century:
454 A case study in Nan Province, Thailand, *Glob Chang Biol*, 24, 4682-4695, 2018b.